






## Revisiting excitation gaps in the fractional quantum Hall effect

Tongzhou Zhao <sup>1</sup>, Koji Kudo <sup>1</sup>, W. N. Faugno <sup>1</sup>, Ajit C. Balram <sup>2,3</sup> and J. K. Jain <sup>1</sup>

<sup>1</sup>*Department of Physics, 104 Davey Lab, Pennsylvania State University, University Park, Pennsylvania 16802, USA*

<sup>2</sup>*Institute of Mathematical Sciences, CIT Campus, Chennai 600113, India*

<sup>3</sup>*Homi Bhabha National Institute, Training School Complex, Anushaktinagar, Mumbai 400094, India*



(Received 15 November 2021; revised 19 May 2022; accepted 23 May 2022; published 31 May 2022)

Recent systematic measurements of the quantum well width dependence of the excitation gaps of fractional quantum Hall states in high mobility samples [Villegas Rosales *et al.*, *Phys. Rev. Lett.* **127**, 056801 (2021)] open the possibility of a better quantitative understanding of this important issue. We present what we believe to be accurate theoretical gaps including the effects of finite width and Landau level (LL) mixing. While theory captures the width dependence, there still remains a deviation between the calculated and the measured gaps, presumably caused by disorder. It is customary to model the experimental gaps of the  $n/(2n \pm 1)$  states as  $\Delta_{n/(2n \pm 1)} = Ce^2/[(2n \pm 1)\epsilon l] - \Gamma$ , where  $\epsilon$  is the dielectric constant of the background semiconductor and  $l$  is the magnetic length; the first term is interpreted as the cyclotron energy of composite fermions and  $\Gamma$  as a disorder-induced broadening of composite-fermion LLs. Fitting the gaps for various fractional quantum Hall states, we find that  $\Gamma$  can be nonzero even in the absence of disorder.

DOI: [10.1103/PhysRevB.105.205147](https://doi.org/10.1103/PhysRevB.105.205147)

### I. INTRODUCTION

It has been appreciated since the very beginning that the existence of a gap is a fundamental property of a fractional quantum Hall effect (FQHE) state [1,2]. Despite the passage of almost four decades, the quantitative agreement between the experimentally measured [3–8] and the theoretically predicted [9–18] values of the gaps is not as good as one might have hoped. In the idealized limit where electrons are in a strict two-dimensional (2D) layer and Landau level (LL) mixing and disorder are absent, comparisons with computer calculations show that the zeroth-order composite fermion (CF) theory predicts gaps of the  $n/(2n \pm 1)$  FQHE states to within 10%, and the agreement can be further improved by allowing for CF-LL mixing [9,19]. The discrepancy between the theoretical and the experimental gaps must, therefore, originate from features not included in the idealized model.

A recent article by Villegas Rosales *et al.* has reported on systematic measurements of the gaps and their quantum well width dependence in the highest mobility samples available to date [8]. The modest aim of our work below is to determine the theoretical values of gaps incorporating, to the best extent we currently know, the effects of finite width and LL mixing (LLM), hoping to gain a better quantitative understanding of this important issue. Our strategy below is first to accurately calculate the thermodynamic limits of the variational gaps with the effect of finite width treated through a local density approximation (LDA); finite width is responsible for the most significant reduction in the gap for typical experimental parameters. We then estimate the thermodynamic limits for the deviation between the variational and the exact gaps in the lowest LL (LLL) and also for correction due to LLM. The final theoretical gaps along with the experimental gaps are shown in Fig. 1. We find that while theory nicely captures the

behavior of the gaps as a function of the quantum well width, a quantitative discrepancy remains, which is most likely due to disorder, not included in our calculations.

We mention here some of the previous theoretical studies of gaps in the FQHE regime. Zhang and Das Sarma [20] calculated finite width correction for the  $1/3$  gap modeling the interaction as  $1/(\sqrt{r^2 + d^2})$ , where  $r$  is the interparticle spacing and  $d$  is related to the width. Park *et al.* [14] evaluated gaps for fractions along the  $n/(2n + 1)$  sequence with a variational Monte Carlo (VMC) method using wave functions from the CF theory, treating finite width in a LDA; they did not go to large widths that have been studied in Ref. [8]. Morf *et al.* [16] evaluated gaps by performing exact diagonalization (ED); they used a Gaussian model for the transverse wave function to simulate the LDA wave function. As for all ED studies, this work is restricted to small systems. Yoshioka [21] calculated the effect of LLM on the  $1/3$  gap by performing ED in the Hilbert space of the two lowest LLs. Melik-Alaverdian and Bonesteel [11] studied the effect of LLM on the energy gap of the  $1/3$  state. They evaluated the quasiparticle energy by diagonalizing the Coulomb interaction in a  $2 \times 2$  basis of the projected and unprojected Jain quasiparticle wave functions; within this approximation, the energies of the ground state and the quasihole are not modified by LLM.

### II. CALCULATIONAL DETAILS

We work with the spherical geometry [22]. In this geometry, a magnetic monopole placed at the center of the sphere generates a uniform radial magnetic flux of strength  $2Qhc/e$  ( $2Q$  is an integer) through the spherical surface, on which  $N$  electrons reside. Owing to the rotational symmetry, states can be characterized by their total orbital angular

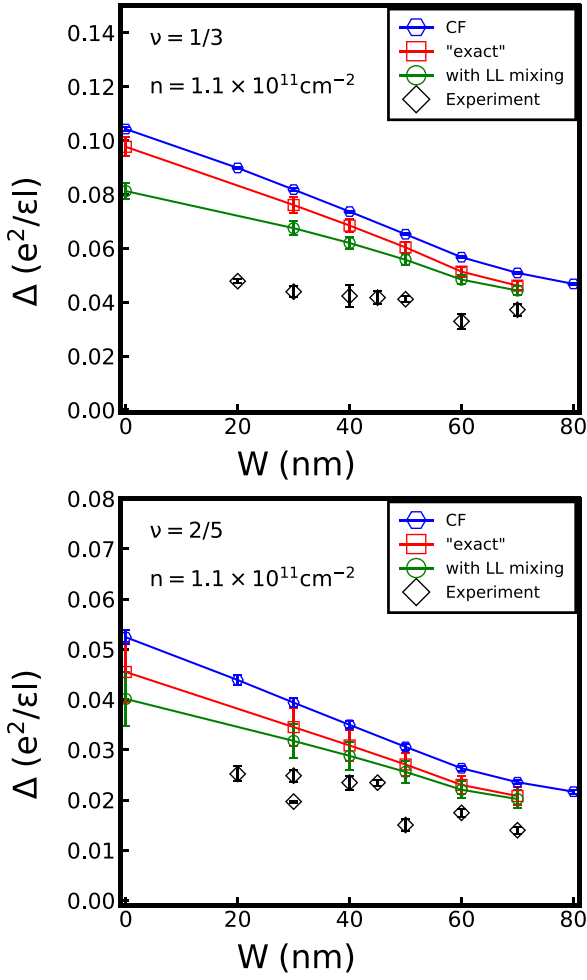


FIG. 1. Comparison between the theoretical and the experimental gaps for  $\rho = 1.1 \times 10^{11} \text{ cm}^{-2}$  at  $\nu = 1/3$  (top) and  $2/5$  (bottom). Several different methods are used for the calculation: VMC with Jain wave functions; VMC gaps corrected for variational error (“exact”), as explained in the main text; LLM corrected gaps (“with LLM”), as explained in the text. Note that an insulating phase is observed in the experiment at  $1/3$  for  $W = 80$  nm.

momentum quantum number  $L$ . Incompressible quantum Hall ground states are uniform, i.e., have  $L = 0$  while their excitations, in general, have  $L > 0$ . Compared with the planar geometry, the flux-particle relationship on the sphere is given by  $2Q = N/\nu - \mathcal{S}$ , where  $\mathcal{S}$  is a topological quantum number called the shift [23]. The planar momentum  $k$  is related to  $L$  as  $k = L/R$ , where  $R = \sqrt{Q}l$  is the radius of the sphere and  $l = \sqrt{\hbar c/eB}$  is the magnetic length at the magnetic-field  $B$ .

The FQHE of electrons at  $\nu = n/(2pn \pm 1)$  is a manifestation of the integer quantum Hall effect (IQHE) of CFs [9,24], which are bound states of electrons and an even number ( $2p$ ) of vortices. The ground-state wave function at these fractions is known to be accurately given by  $\Psi_{n/(2n+1)}^{\text{Jain}} = \mathcal{P}_{\text{LLL}} \Phi_n \Phi_1^2$ , where  $\Phi_n$  is the IQHE wave function of electrons at filling factor  $n$  and  $\mathcal{P}_{\text{LLL}}$  implements projection to the LLL as is appropriate in the limit that  $B \rightarrow \infty$ . Throughout this work, we carry out the LLL projection using the Jain-Kamilla method, details of which can be found in the literature [9,13,25]. The

lowest-energy neutral excitation is obtained by promoting a CF from the highest occupied  $\Lambda L$  to the lowest unoccupied  $\Lambda L$ . The wave function for this state, termed the CF exciton (CFE), is given by  $\Psi_{n/(2n+1)}^{\text{CFE}} = \mathcal{P}_{\text{LLL}} \Phi_n^{\text{ex}} \Phi_1^2$ , where  $\Phi_n^{\text{ex}}$  is the IQHE wave function of an exciton with a hole in the LL indexed by  $n - 1$  and a particle in the LL indexed by  $n$ . The constituent quasiparticle and quasihole of the CFE are referred to as the CF particle (CFP) and CF hole (CFH). The gap measured in transport corresponds to the energy of a far separated CFP-CFH pair. In the spherical geometry, at  $\nu = n/(2n + 1)$  this state is obtained by placing the CFH and the CFP at the north and south poles, respectively, which corresponds to the CFE with the largest  $L_{\text{max}} = (N - n^2)/n + (2n - 1)$  [17]. The detailed form of the above wave functions in the spherical geometry is given in the Supplemental Material (SM) [26].

To calculate the transport gap accurately, the attractive interaction between the CFH and the CFP that exists in any finite system needs to be accounted for. The CFP and CFH have an extent of only a few magnetic lengths [27], so in the simplest approximation, we treat them as point particles with charge  $(\pm e)/(2n + 1)$  [9] separated by a distance of  $2\sqrt{Q}l$ , which is the diameter of the sphere. The resulting Coulomb attraction between the CFP and the CFH is thus given by

$$V_{\text{CFH-CFP}} = -\frac{1}{(2n + 1)^2 (2\sqrt{Q})} \frac{e^2}{\epsilon l}. \quad (1)$$

Taking this attractive interaction into account, we define the transport gap as

$$\Delta = \sqrt{\frac{2Q\nu}{N}} (E_{\text{CFE}}^{L_{\text{max}}} - E_{\text{gs}} - V_{\text{CFH-CFP}}), \quad (2)$$

where  $E_{\text{CFE}}^{L_{\text{max}}}$  and  $E_{\text{gs}}$  are the expectation values of the Coulomb energies of the wave functions corresponding to the largest- $L$  CFE and ground state, respectively. The expectation values for the variational wave functions are evaluated using the Metropolis Monte Carlo method. In Eq. (2) the factor of  $\sqrt{2Q\nu}/N$  corrects for the density difference between a finite system on the sphere and that in the thermodynamic limit and thereby reduces the  $N$  dependence of the gaps [28].

To compare the theoretical gaps against the experimental values, we need to carefully incorporate the effect of the finite width of the quantum well. To do so we consider the effective interaction given by

$$V_{\text{eff}}(r) = \frac{e^2}{\epsilon} \int d\xi_1 \int d\xi_2 \frac{|\psi(\xi_1)|^2 |\psi(\xi_2)|^2}{\sqrt{r^2 + (\xi_1 - \xi_2)^2}}, \quad (3)$$

where  $r$  is the in-plane distance between two particles,  $\xi$  is the transverse coordinate, and  $\psi(\xi)$  is the transverse wave function which is obtained from a separate LDA calculation [29].

### III. LLM: PERTURBATIVE APPROACH

One of our objectives is to determine the modification of the gap due to LLM. The LLM parameter  $\kappa$ , defined as  $\kappa = (e^2/\epsilon l)/(\hbar\omega_c)$ , characterizes the strength of the Coulomb interaction relative to the cyclotron energy, where  $\omega_c = eB/m_b c$  is the cyclotron frequency of the band electron, where  $m_b$  is the band mass. To study the effect of LLM, we carry out ED

using a perturbative method that incorporates LLM through a correction to the interaction (including a three-body interaction) [30–33].

The effective Hamiltonian we use is given by  $\hat{V}_c(W) + \kappa[\hat{V}_2(W) + \hat{V}_3(W)]$ , where  $\hat{V}_c(W)$  is the Coulomb interaction for a quantum well of width  $W$ ,  $\kappa\hat{V}_2(W)$  is the correction to the two-body interaction due to LLM, and  $\kappa\hat{V}_3(W)$  is the three-body interaction term generated by LLM. In the disk geometry, these have the form

$$\hat{V}_c(W) = \sum_{m=0}^{\infty} V_c(W, m) \sum_{i < j} P_{ij}(m), \quad (4)$$

$$\hat{V}_2(W) = \sum_{m=0}^{m_{2,\max}} V_2(W, m) \sum_{i < j} P_{ij}(m),$$

$$\hat{V}_3(W) = \sum_{m=0}^{m_{3,\max}} V_3(W, m) \sum_{i < j < k} P_{ijk}(m),$$

where  $P_{ij}(m)$  and  $P_{ijk}(m)$  are the projection operators onto a pair or a triplet of electrons, respectively, with relative angular momentum  $m$ . The pseudopotential  $V_c(W, m)$  is given by [34].

$$V_c(W, m) = \int_0^{\infty} dk k [L_0(k^2/2)]^2 L_m(k^2) e^{-k^2} V(k) \quad (5)$$

$$V(k) = \frac{e^2 l}{\epsilon k} \frac{3kW + \frac{8\pi^2}{kW} - \frac{32\pi^4(1-e^{-kW})}{(kW)^2[(kW)^2 + 4\pi^2]}}{(kW)^2 + 4\pi^2}, \quad (6)$$

where  $k$  is quoted in units of  $1/l$ . As for  $V_2(W, m)$  and  $V_3(W, m)$ , we use the values quoted in Tables I and II of Ref. [31] {the corrections up to  $m_{2,\max} = 8$  and  $m_{3,\max} = 8$  are given in Ref. [31] and thus we truncate the sums in Eq. (4) to these values}. (It is noted that these values are obtained for a transverse wave function of the cosine form. We make the simplifying assumption below that the LLM reduction factor is not strongly sensitive to the form of the transverse wave function.) Using these planar disk pseudopotentials in the spherical geometry, we compute the energy gap of a far separated CFP-CFH pair as defined in Eq. (2) using ED. In the following calculations, we set  $\kappa = 0.70$  and  $0.76$  at  $\nu = 1/3$  and  $2/5$ , respectively, as appropriate for the experiments of Ref. [8], with electron density  $\rho = 1.1 \times 10^{11} \text{ cm}^{-2}$ .

In Fig. 2, we plot the energy gaps at  $\nu = 1/3$  and  $\nu = 2/5$  for  $W = 0$  as functions of the inverse of the particle number. The energy gaps for the interaction  $\hat{V}_c + \kappa[\hat{V}_2 + \hat{V}_3]$  are always smaller than those for  $\hat{V}_c$  at any  $N$  since LLM screens the interaction. Figure 3 shows LLM reduction factor  $r \equiv \Delta_{V_c + \kappa[V_2 + V_3]} / \Delta_{V_c}$ , which is the ratio of the gaps with and without LLM, as a function of  $1/N$  for several quantum well widths. We deduce the value in the thermodynamic limit for each  $W/l$  by linear extrapolation. Using these data, we generate Fig. 4 that plots the reduction factor  $r$  as a function of  $W$ . Here we set the magnetic length as  $l = \sqrt{\nu/(2\pi\rho)}$  with  $\rho = 1.1 \times 10^{11} \text{ cm}^{-2}$ . Because the interelectron interaction weakens with increasing width, we expect the effect of LLM to become less prominent, which is consistent with the finding that the reduction in gap decreases with increasing quantum well width.

In the SM [26], we discuss an alternative approach for treating LLM, namely, the fixed-phase diffusion Monte Carlo

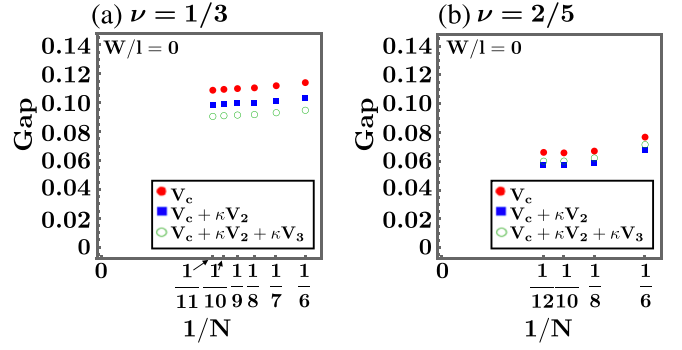


FIG. 2. Energy gap [defined in Eq. (2)] incorporating the effect of LLM [see Eq. (4)] as a function of the inverse of the particle number at (a)  $\nu = 1/3$  and (b)  $\nu = 2/5$  obtained from ED in the spherical geometry.

method, which has proved to be effective in dealing with the effect of LLM in the context of competition between FQHE states with different spins and also between liquid and crystal states [35–39]. We believe that this method may underestimate LLM corrections to gaps because fixing the phase of the wave function limits the flexibility of the CFP and CFH wave functions. Also, this method allows a determination of LLM corrections only for zero width; for finite widths, the thermodynamic extrapolations are not reliable.

#### IV. RESULTS AND DISCUSSION

We evaluate the gaps as follows. First, we determine the thermodynamic limits for the gaps at filling fractions  $1/3$ ,  $2/5$ ,  $3/7$ ,  $4/9$ , and  $5/11$  from the Jain wave functions for the ground states and far separated quasiparticle-quasihole pair. We then estimate the thermodynamic limit of the “variational error,” namely, the discrepancy between the gaps from trial wave functions of the CF theory and ED; this can be accomplished reliably for  $1/3$  and  $2/5$  but not for the other fractions for which the number of systems on which ED can be performed is not sufficient for a thermodynamic extrapolation. Finally, we multiply the gap by the reduction factor obtained above to include the effect of LLM.

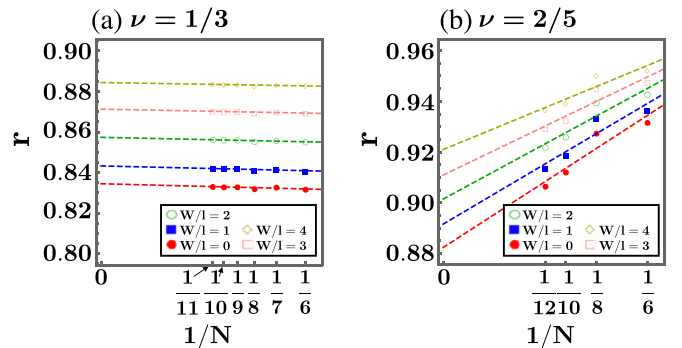


FIG. 3. The reduction factor  $r$  as a function of  $1/N$  for (a)  $\nu = 1/3$  and (b)  $\nu = 2/5$ . The reduction factor  $r$  is defined as the ratio of the gap for  $\hat{V}_c + \kappa[\hat{V}_2 + \hat{V}_3]$  (which includes LLM) to the gap for the bare Coulomb interaction  $\hat{V}_c$ . The dashed lines represent a linear approximation.

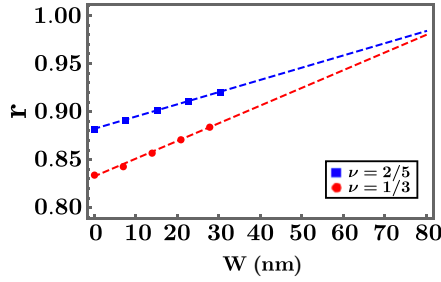


FIG. 4. The reduction factor  $r$  as a function of  $W$ , where  $r$  is the factor by which the gap is reduced due to LLM. The dashed lines represent a linear approximation.

The resulting gaps for  $1/3$  and  $2/5$  states are shown in Fig. 1 as a function of the quantum well width  $W$  for density  $\rho = 1.1 \times 10^{11} \text{cm}^{-2}$ . The blue symbols show the thermodynamic limits of the VMC gaps (labeled VMC). Evidently, finite width causes the largest correction to the gap. The red symbols are gaps corrected for the variational error. Comparisons with ED studies have shown (see overlaps shown in Refs. [18,26,38]) that the Laughlin and Jain trial wave functions for the  $1/3$ ,  $2/5$ , and  $3/7$  ground states remain very accurate even for finite widths; we find that the use of these trial wave functions overestimates the gaps by  $\sim 10\%$  (the estimation of this error is primarily responsible for the uncertainty in the theoretical gaps). The green dashed line is obtained by multiplying the gaps by the reduction factor  $r$  given in Fig. 4 to include corrections due to LLM. This is the primary result of our calculation. We note that the theoretical and experimental gaps behave qualitatively similarly, and the discrepancy between them, presumably attributable to disorder, is only weakly dependent on the quantum well width. For  $\nu = 2/5$  the deviation between theory and experiment is of the same order as the scatter in the experimental gaps. Given various approximations in the model and the calculations, we find this level of agreement to be satisfactory.

We next come to the behavior of gaps as a function of the filling factor. In the zeroth-order approximation of noninteracting CFs, it is natural to interpret the gaps in terms of the CF cyclotron energy  $\hbar e B^* / m^* c$ , where  $B^*$  is the effective magnetic field sensed by CFs and  $m^*$  is their mass. This suggests that the gap is proportional to  $[1/(2n \pm 1)](e^2/\epsilon l)$ , where  $\epsilon$  is the dielectric constant of the background semiconductor and  $l = \sqrt{\hbar c / e B}$  is the magnetic length. This follows from the observations that for the  $\nu = n/(2n \pm 1)$  state we have  $B^* = B/(2n \pm 1)$ , and that we must have  $m^* \propto \sqrt{B}$  for the gap to be proportional to the Coulomb energy  $e^2/\epsilon l$ , the only energy scale in the absence of LLM. Experimental gaps can be fitted, approximately, to

$$\Delta_{n/(2n \pm 1)} = \frac{C}{2n \pm 1} \frac{e^2}{\epsilon l} - \Gamma, \quad (7)$$

where  $C$  and  $\Gamma$  are constants that are determined by the fitting. The quantity  $\Gamma$  is often interpreted as a disorder-induced broadening of CF-LLs, known as  $\Lambda$  levels ( $\Lambda$ LS). Many experiments have reported values for  $\Gamma$  [6,8].

Villegas Rosales *et al.* estimate  $\Gamma$  in Eq. (7) to be in the range  $0.005 - 0.02 e^2/\epsilon l$  [8], with the precise value depend-

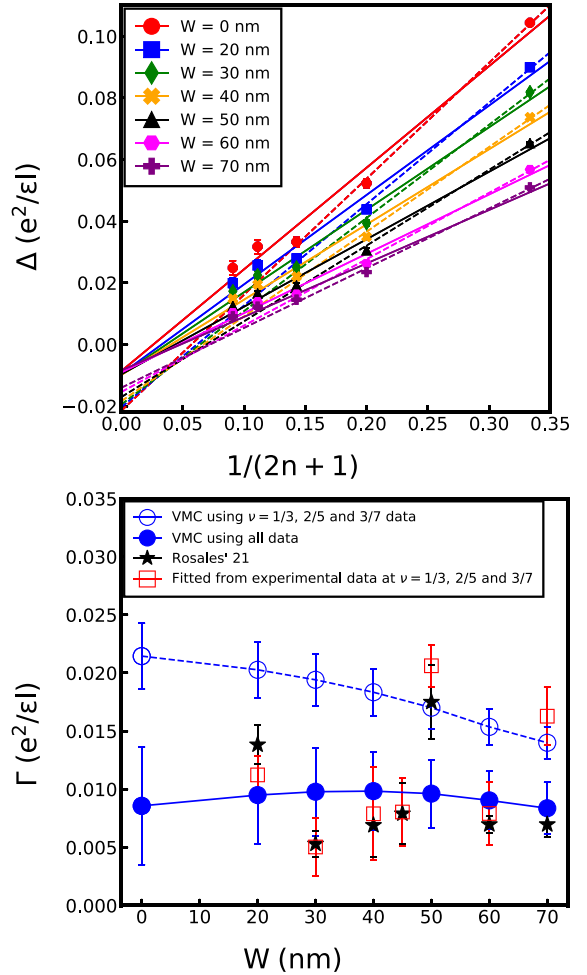


FIG. 5. Top panel: Theoretical transport gap  $\Delta$  as a function of  $1/(2n + 1)$  for state in the  $n/(2n + 1)$  sequence in GaAs quantum wells at different widths  $W$  with density  $\rho = 1.1 \times 10^{11} \text{cm}^{-2}$ . The gap is calculated using the VMC method. Different markers correspond to different well widths. The solid lines are fits using data points at all filling factors while the dashed lines are fits of the gaps at only  $\nu = 1/3, 2/5$  and  $3/7$ . Bottom panel: Comparison between  $\Gamma$  from the VMC gaps with its experimentally measured value as a function of the well width for density  $\rho = 1.1 \times 10^{11} \text{cm}^{-2}$ . The blue solid circles are obtained by linear regression of data points at all filling factors ( $\nu = 1/3, 2/5, 3/7, 4/9$  and  $5/11$ ), which correspond to solid lines in the top plot, while the blue hollow circles are obtained by linear regression of gaps only for  $\nu = 1/3, 2/5$  and  $3/7$ , which correspond to dashed lines in the top plot. The black stars are directly taken from Fig. 5 of Ref. [8] and the red squares are obtained from a linear fit of the experimental data at  $\nu = 1/3, 2/5, 3/7$  in Ref. [8].

ing on the quantum well width. Traditionally, a nonzero  $\Gamma$  has been attributed to the disorder-induced broadening of the  $\Lambda$  levels [6]. In Fig. 5 we plot the theoretical VMC gaps for  $1/3, 2/5, 3/7, 4/9$ , and  $5/11$  states without including the effects of the disorder, LLM, or variational error (which are difficult to estimate for the higher-order fractions). We find that if we attempt a linear fit, the gaps are approximately consistent with Eq. (7) with a *nonzero*  $\Gamma$  for typical widths of the quantum well (a similar behavior was noted in Ref. [14], but with a less realistic treatment of finite width). This value of  $\Gamma$  depends on

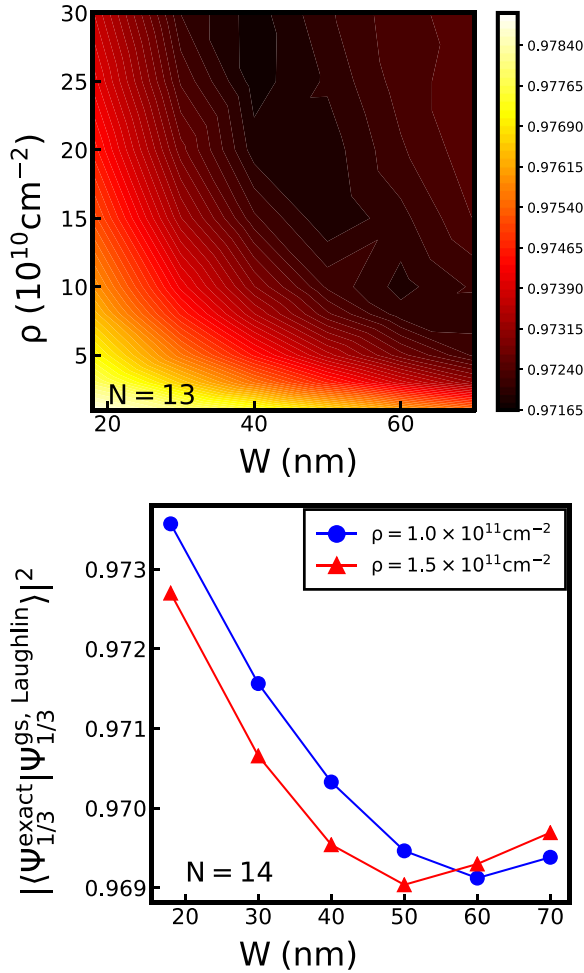


FIG. 6. Squared overlaps of the exact ground states with the Laughlin state at  $\nu = 1/3$  for  $N = 13$  (upper panel) and  $N = 14$  (lower panel) electrons in the spherical geometry. The plot for  $N = 14$  only includes data at  $\rho = 1.0 \times 10^{11} \text{cm}^{-2}$  and  $\rho = 1.5 \times 10^{11} \text{cm}^{-2}$ . The exact ground states are evaluated using the pseudopotentials of the finite-width interaction.

the range of fractions used for the fit; we show fits using the gaps at  $1/3$ ,  $2/5$ , and  $3/7$  (which are known more precisely), as well as fits using all of the gaps. The resulting  $\Gamma$  is in the same range as that seen experimentally [8]. Moreover, in the experiments of Villegas Rosales *et al.* [8], there is no clear correlation between the measured  $\Gamma$  and the sample mobility which characterizes the disorder strength further suggesting that  $\Gamma$  may not be attributable solely to disorder. The implications of these results to the CF mass, which is related to the gaps, are discussed in the SM [26], which also includes many other details.

One may also ask how robust the FQHE states are as the width is increased. The ED study in Ref. [38] has shown that the overlap of the  $N = 12$  exact state with the Laughlin wave function at  $1/3$  is very close to unity even in wide quantum wells. In this paper, we extend their result by calculating the overlap between the exact ground state and the Laughlin state for  $N = 13, 14$  at  $\nu = 1/3$  for quantum well widths ranging from 0 to 70 nm and carrier densities ranging from  $10^{10} \text{cm}^{-2}$

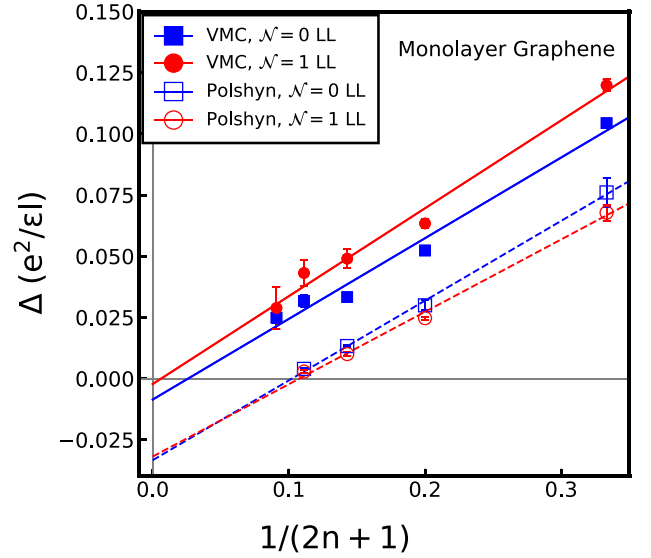


FIG. 7. Theoretical transport gap  $\Delta$  as a function of  $1/(2n+1)$  for states at filling factors  $|\nu| = n/(2n+1)$  sequence in the  $\mathcal{N} = 0$  and  $\mathcal{N} = 1$  LLs of graphene. The solid blue squares and red circles are activation gaps obtained from the (VMC method without including the effects of LLM). The hollow symbols are the experimental gaps measured by Polshyn *et al.* [43]. The solid lines are fitted from the VMC gap data at all filling factors ( $1/3$ ,  $2/5$ ,  $3/7$ ,  $4/9$  and  $5/11$ ), and the dashed lines are fitted from the experimental gaps at all filling factors ( $1/3$ ,  $2/5$ ,  $3/7$  and  $4/9$ ).

to  $3 \times 10^{11} \text{cm}^{-2}$ . These overlaps are shown in Fig. 6. We find that for these larger systems too, the  $\nu = 1/3$  Laughlin wave function provides an almost exact representation of the ground states for the entire range of widths and densities considered in our work. This indicates, theoretically, that this state survives until a first-order transition takes place into a compressible liquid or crystal bilayer state [40,41] (experimentally to an insulating state [42]). This is consistent with the rather sudden collapse of the  $1/3$  state observed experimentally as a function of the quantum well width [8]. We expect that the same remains true for other prominent FQHE states.

Finally, we ask how these considerations apply to FQHE in graphene. A similar analysis has been performed for the gaps in monolayer graphene by Polshyn *et al.* [43]. They find that  $\Gamma$  is larger by a factor of  $\sim 3$  than that seen in GaAs quantum wells. The measured gaps are shown in Fig. 7. [We show the gaps at  $\nu = -1 + n/(2n+1)$  in the  $\mathcal{N} = 0$  graphene LL, and the gaps at  $\nu = -3 + n/(2n+1)$  in the  $\mathcal{N} = 1$  graphene LL, because these are the largest experimental gaps.] For the  $\mathcal{N} = 0$  graphene LL, the theoretical gaps are identical to those in the LLL of GaAs in the zero-width limit, when LLM is neglected [44]. Earlier studies have demonstrated that the CF theory is quantitatively accurate in the  $\mathcal{N} = 1$  graphene LL [45,46]. We have evaluated the VMC activation gaps for the FQHE states at  $\nu = n/(2n+1)$  in the  $\mathcal{N} = 1$  LL of graphene using the effective interaction given in Ref. [45] (see SM). The results are also shown in Fig. 7. It is not known at present how much LLM and disorder contribute to the observed value of  $\Gamma$  in experiments.

In summary, motivated by the recent experimental study of gaps of various FQHE states in extremely high mobility

systems, we have evaluated the excitation gaps including the effects of finite width and LLM. The theoretical gaps are in qualitative and semi-quantitative agreement with the experimental gaps, but some discrepancy remains, presumably due to disorder.

### ACKNOWLEDGMENTS

We are grateful to Mansour Shayegan for many insightful discussions and for raising the questions that motivated this work and to G. J. Sreejith for help with interaction pseudopotentials. T.Z., W.N.F., and J.K.J. acknowledge financial support from the U.S. Department of Energy under

Award No. DE-SC-0005042. K.K. thanks JSPS for support from Overseas Research Fellowship for Research Abroad. A.C.B. acknowledges the Science and Engineering Research Board (SERB) of the Department of Science and Technology (DST) for funding support via the Start-up Grant SRG/2020/000154. The numerical calculations were performed using Advanced CyberInfrastructure computational resources provided by The Institute for CyberScience at The Pennsylvania State University and the Nandadevi supercomputer, which is maintained and supported by the Institute of Mathematical Science's High-Performance Computing Center. Some of the computations were performed using the AQILA [29] and DiagHam packages, for which we are grateful to its authors.

- 
- [1] D. C. Tsui, H. L. Stormer, and A. C. Gossard, Two-Dimensional Magnetotransport in the Extreme Quantum Limit, *Phys. Rev. Lett.* **48**, 1559 (1982).
- [2] R. B. Laughlin, Anomalous Quantum Hall Effect: An Incompressible Quantum Fluid with Fractionally Charged Excitations, *Phys. Rev. Lett.* **50**, 1395 (1983).
- [3] G. S. Boebinger, A. M. Chang, H. L. Stormer, and D. C. Tsui, Magnetic Field Dependence of Activation Energies in the Fractional Quantum Hall Effect, *Phys. Rev. Lett.* **55**, 1606 (1985).
- [4] R. L. Willett, H. L. Stormer, D. C. Tsui, A. C. Gossard, and J. H. English, Quantitative experimental test for the theoretical gap energies in the fractional quantum Hall effect, *Phys. Rev. B* **37**, 8476 (1988).
- [5] M. Shayegan, J. Jo, Y. W. Suen, M. Santos, and V. J. Goldman, Collapse of the Fractional Quantum Hall Effect in an Electron System with Large Layer Thickness, *Phys. Rev. Lett.* **65**, 2916 (1990).
- [6] R. R. Du, H. L. Stormer, D. C. Tsui, L. N. Pfeiffer, and K. W. West, Experimental Evidence for New Particles in the Fractional Quantum Hall Effect, *Phys. Rev. Lett.* **70**, 2944 (1993).
- [7] W. Pan, W. Kang, M. P. Lilly, J. L. Reno, K. W. Baldwin, K. W. West, L. N. Pfeiffer, and D. C. Tsui, Particle-Hole Symmetry and the Fractional Quantum Hall Effect in the Lowest Landau Level, *Phys. Rev. Lett.* **124**, 156801 (2020).
- [8] K. A. Villegas Rosales, P. T. Madathil, Y. J. Chung, L. N. Pfeiffer, K. W. West, K. W. Baldwin, and M. Shayegan, Fractional Quantum Hall Effect Energy Gaps: Role of Electron Layer Thickness, *Phys. Rev. Lett.* **127**, 056801 (2021).
- [9] J. K. Jain, *Composite Fermions* (Cambridge University Press, New York, 2007).
- [10] F. D. M. Haldane and E. H. Rezayi, Finite-Size Studies of the Incompressible State of the Fractionally Quantized Hall Effect and its Excitations, *Phys. Rev. Lett.* **54**, 237 (1985).
- [11] V. Melik-Alaverdian and N. E. Bonesteel, Composite fermions and Landau-level mixing in the fractional quantum Hall effect, *Phys. Rev. B* **52**, R17032 (1995).
- [12] M. W. Ortalano, S. He, and S. Das Sarma, Realistic calculations of correlated incompressible electronic states in GaAs- $\text{Al}_x\text{Ga}_{1-x}$  as heterostructures and quantum wells, *Phys. Rev. B* **55**, 7702 (1997).
- [13] J. K. Jain and R. K. Kamilla, Composite fermions in the Hilbert space of the lowest electronic Landau level, *Int. J. Mod. Phys. B* **11**, 2621 (1997).
- [14] K. Park, N. Meskini, and J. Jain, Activation gaps for the fractional quantum Hall effect: realistic treatment of transverse thickness, *J. Phys.: Condens. Matter* **11**, 7283 (1999).
- [15] V. W. Scarola, S.-Y. Lee, and J. K. Jain, Excitation gaps of incompressible composite fermion states: Approach to the Fermi sea, *Phys. Rev. B* **66**, 155320 (2002).
- [16] R. H. Morf, N. d'Ambrumenil, and S. Das Sarma, Excitation gaps in fractional quantum Hall states: An exact diagonalization study, *Phys. Rev. B* **66**, 075408 (2002).
- [17] A. C. Balram and S. Pu, Positions of the magnetoroton minima in the fractional quantum Hall effect, *Eur. Phys. J. B* **90**, 124 (2017).
- [18] A. C. Balram and A. Wójs, Fractional quantum Hall effect at  $\nu = 2 + 4/9$ , *Phys. Rev. Res.* **2**, 032035(R) (2020).
- [19] A. C. Balram, A. Wójs, and J. K. Jain, State counting for excited bands of the fractional quantum Hall effect: Exclusion rules for bound excitons, *Phys. Rev. B* **88**, 205312 (2013).
- [20] F. C. Zhang and S. Das Sarma, Excitation gap in the fractional quantum Hall effect: Finite layer thickness corrections, *Phys. Rev. B* **33**, 2903 (1986).
- [21] D. Yoshioka, Effect of the Landau level mixing on the ground state of two-dimensional electrons, *J. Phys. Soc. Jpn.* **53**, 3740 (1984).
- [22] F. D. M. Haldane, Fractional Quantization of the Hall Effect: A Hierarchy of Incompressible Quantum Fluid States, *Phys. Rev. Lett.* **51**, 605 (1983).
- [23] X. G. Wen and A. Zee, Shift and Spin vector: New topological quantum numbers for the Hall fluids, *Phys. Rev. Lett.* **69**, 953 (1992).
- [24] J. K. Jain, Composite-fermion approach for the fractional quantum Hall effect, *Phys. Rev. Lett.* **63**, 199 (1989).
- [25] J. K. Jain and R. K. Kamilla, Quantitative study of large composite-fermion systems, *Phys. Rev. B* **55**, R4895 (1997).
- [26] See Supplemental Material at <http://link.aps.org/supplemental/10.1103/PhysRevB.105.205147> for details of (i) the trial-wave functions we use to evaluate the gaps; (ii) the VMC results at densities and filling factors other than those presented in the

- main text; (iii) the estimation of the different corrections, i.e, from the use of variational wave functions and LL mixing; (iv) the estimate of the CF masses from the gaps; and (v) gaps in the first excited LL of graphene, which includes Refs. [47–52].
- [27] A. C. Balram, Y.-H. Wu, G. J. Sreejith, A. Wójs, and J. K. Jain, Role of Exciton Screening in the  $\nu = 7/3$  Fractional Quantum Hall Effect, *Phys. Rev. Lett.* **110**, 186801 (2013).
- [28] R. Morf, N. d’Ambrumenil, and B. I. Halperin, Microscopic wave functions for the fractional quantized Hall states at  $\nu = \frac{2}{5}$  and  $\frac{2}{7}$ , *Phys. Rev. B* **34**, 3037 (1986).
- [29] M. Rother, 2D Schroedinger Poisson solver AQILA, <https://www.mathworks.com/matlabcentral/fileexchange/3344-2d-schroedinger-poisson-solver-aquila> (2009–2020).
- [30] W. Bishara and C. Nayak, Effect of Landau level mixing on the effective interaction between electrons in the fractional quantum Hall regime, *Phys. Rev. B* **80**, 121302(R) (2009).
- [31] M. R. Peterson and C. Nayak, More realistic Hamiltonians for the fractional quantum Hall regime in GaAs and graphene, *Phys. Rev. B* **87**, 245129 (2013).
- [32] M. R. Peterson and C. Nayak, Effects of Landau Level Mixing on the Fractional Quantum Hall Effect in Monolayer Graphene, *Phys. Rev. Lett.* **113**, 086401 (2014).
- [33] I. Sodemann and A. H. MacDonald, Landau level mixing and the fractional quantum Hall effect, *Phys. Rev. B* **87**, 245425 (2013).
- [34] S. Das Sarma and B. A. Mason, Optical phonon interaction effects in layered semiconductor structures, *Ann. Phys.* **163**, 78 (1985).
- [35] G. Ortiz, D. M. Ceperley, and R. M. Martin, New Stochastic Method for Systems with Broken Time-Reversal Symmetry: 2D Fermions in a Magnetic Field, *Phys. Rev. Lett.* **71**, 2777 (1993).
- [36] J. Zhao, Y. Zhang, and J. K. Jain, Crystallization in the Fractional Quantum Hall Regime Induced by Landau-Level Mixing, *Phys. Rev. Lett.* **121**, 116802 (2018).
- [37] Y. Zhang, A. Wójs, and J. K. Jain, Landau-Level Mixing and Particle-Hole Symmetry Breaking for Spin Transitions in the Fractional Quantum Hall Effect, *Phys. Rev. Lett.* **117**, 116803 (2016).
- [38] T. Zhao, W. N. Faugno, S. Pu, A. C. Balram, and J. K. Jain, Origin of the  $\nu = 1/2$  fractional quantum Hall effect in wide quantum wells, *Phys. Rev. B* **103**, 155306 (2021).
- [39] M. S. Hossain, T. Zhao, S. Pu, M. A. Mueed, M. K. Ma, K. A. V. Rosales, Y. J. Chung, L. N. Pfeiffer, K. W. West, K. W. Baldwin *et al.*, Bloch ferromagnetism of composite fermions, *Nat. Phys.* **17**, 48 (2021).
- [40] V. W. Scarola and J. K. Jain, Phase diagram of bilayer composite fermion states, *Phys. Rev. B* **64**, 085313 (2001).
- [41] W. N. Faugno, A. J. Duthie, D. J. Wales, and J. K. Jain, Exotic bilayer crystals in a strong magnetic field, *Phys. Rev. B* **97**, 245424 (2018).
- [42] Y. W. Suen, H. C. Manoharan, X. Ying, M. B. Santos, and M. Shayegan, Origin of the  $\nu = 1/2$  fractional Quantum Hall State in Wide Single Quantum Wells, *Phys. Rev. Lett.* **72**, 3405 (1994).
- [43] H. Polshyn, H. Zhou, E. M. Spanton, T. Taniguchi, K. Watanabe, and A. F. Young, Quantitative Transport Measurements of Fractional Quantum Hall Energy Gaps in Edgeless Graphene Devices, *Phys. Rev. Lett.* **121**, 226801 (2018).
- [44] A. C. Balram, C. Töke, A. Wójs, and J. K. Jain, Fractional quantum Hall effect in graphene: Quantitative comparison between theory and experiment, *Phys. Rev. B* **92**, 075410 (2015).
- [45] A. C. Balram, C. Töke, A. Wójs, and J. K. Jain, Spontaneous polarization of composite fermions in the  $n = 1$  Landau level of graphene, *Phys. Rev. B* **92**, 205120 (2015).
- [46] A. C. Balram, Transitions from Abelian composite fermion to non-Abelian parton fractional quantum Hall states in the zeroth Landau level of bilayer graphene, *Phys. Rev. B* **105**, L121406 (2022).
- [47] P. J. Reynolds, J. Tobochnik, and H. Gould, Diffusion quantum monte carlo, *Comput. Phys.* **4**, 662 (1990).
- [48] R. Du, H. Stormer, D. Tsui, L. Pfeiffer, and K. West, Shubnikov-dehaas oscillations around  $\nu = 1/2$  Landau level filling factor, *Solid State Commun.* **90**, 71 (1994).
- [49] P. T. Coleridge, Z. W. Wasilewski, P. Zawadzki, A. S. Sachrajda, and H. A. Carmona, Composite-fermion effective masses, *Phys. Rev. B* **52**, R11603 (1995).
- [50] J. K. Jain and R. K. Kamilla, Composite fermions: Particles of the lowest Landau level, in *Composite Fermions* (World Scientific Pub Co Inc., Singapore, 1998), Chap. 1, pp. 1–90.
- [51] L. Mitas, Diffusion Monte Carlo, in *Quantum Monte Carlo Methods in Physics and Chemistry*, edited by M. P. Nightingale and C. J. Umrigar, Nato Science Series C: Vol. 525 (Kluwer, Academic Publishers, Dordrecht, The Netherlands, 1999), pp. 247–261.
- [52] W. M. C. Foulkes, L. Mitas, R. J. Needs, and G. Rajagopal, Quantum Monte Carlo simulations of solids, *Rev. Mod. Phys.* **73**, 33 (2001).